CRYSTAL GROWTH & DESIGN

Article

pubs.acs.org/crystal

Generating Ionic Liquids from Ionic Solids: An Investigation of the Melting Behavior of Binary Mixtures of Ionic Liquids

Guilherme J. Maximo,[†,‡] Ricardo J. B. N. Santos,[‡] Paula Brandão,[‡] José M. S. S. Esperança,[§] Mariana C. Costa,[∥] Antonio J. A. Meirelles,[†] Mara G. Freire,[‡] and João A. P. Coutinho*[,‡]

[†]Laboratory of Extraction, Applied Thermodynamics and Equilibrium, School of Food Engineering, University of Campinas, Campinas, São Paulo, Brazil

[‡]Chemistry Department, CICECO, University of Aveiro, Aveiro, Portugal

[§]Instituto de Tecnologia Química e Biológica, Universidade Nova de Lisboa, Oeiras, Portugal

[∥]School of Applied Sciences, University of Campinas, Limeira, São Paulo, Brazil

S *Supporting Information*

ABSTRACT: Mixtures of ionic liquids (ILs) allow enlarging the plethora of the physical and chemical properties of these materials in addition to the well-known tunable character associated with pure compounds. It is shown here that mixtures also induce a significant decrease of the melting points of the mixture to values well below those of the original compounds allowing the tuning of the melting point of an ionic liquid mixture and the generation of novel ionic liquids from mesotherm salts. This work evaluates the melting behavior of mixtures of seven hexafluorophosphate-based compounds combined with imidazolium-, pyridinium-, pyrrolidinium-, piperidinium- ammonium-, or phosphonium-based cations. The solid−liquid equilibrium phase diagrams of nine of their binary mixtures were measured using optical microscopy and differential scanning calorimetry. The pure ILs' melting profile reveals the presence of polymorphs with highly energetic solid−solid transitions that are relevant for the evaluation of these systems. The phase diagrams reported here also allow an investigation on the nonideality of the mixtures of ionic liquids. A classical thermodynamic approach shows that while most of the mixtures investigated present an ideal liquid behavior, others show slight or even marked nonideal profiles. One particular system, [C_3mpyr][PF_6] (1-methyl-1-propylpyrrolidinium hexafluorophosphate) + [C_3mpip][PF_6] (1-methyl-1-propylpiperidinium hexafluorophosphate), displays a continuous solid solution as established by differential scanning calorimetry, powder X-ray diffraction, and crystallographic data being one of the few ionic liquid alloys ever reported.

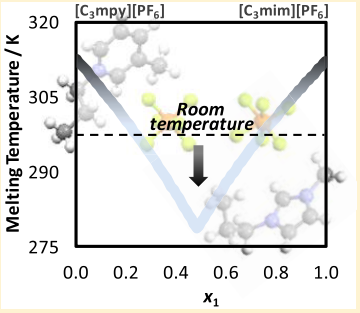

INTRODUCTION

Ionic liquids (ILs) are salts whose melting point is lower than 100 °C. This is an arbitrary definition based on the water boiling point, and a large number of mesotherm salts, i.e., salts with a higher melting point yet chemically similar to ionic liquids, fail to meet this criterion and seem to be excluded from the ILs realm. Yet the low melting point is, in many cases, relevant as it expands their liquid phase domain, and so their applicability, while maintaining the particular chemical characteristics of ionic substances.[1,2] Being salts, they can have their properties tuned by the adequate choice of a large range of cation−anion pairs. The tunability of these materials that is at the basis of the "designer solvent" concept can be further expanded by the use of IL mixtures that may further enhance the possibilities of optimization of their properties.

Researchers working on the ILs field started recently, though still tenuously, to evaluate the use of binary or ternary mixtures of ILs.[3] Among other advantages, the mixing of two compounds can lead to a melting temperature depression until a minimum value when melting occurs without phase separation: the eutectic point. Thenceforth, with the continuous addition of one of the compounds, the mixture's melting point starts to increase again. The great interest in this kind of mixture is that a system can be formulated so that two ionic solids can be mixed to give a eutectic mixture that is liquid at, or close to, room temperature operating conditions. In order to reach such a target, the salt systems' melting profile can be modified through the right choice of a cation−anion pair, manipulating the size and shape of their chemical structures and changing the repulsive/attractive forces that build the lattice energy of the solid state.[4,5] In this way, it is possible to enlarge the options for materials design using ionic compounds and to produce ILs from non-ILs[6] for a variety of applications, such as stationary phases for chromatography columns,[7] processing of cellulose[8] and preparation of cellulose nanofibers,[9] heterogeneous catalysts,[10] batteries and solar energy appliances,[11,12] heat transfer-storage processes,[13] design of anion-exchange membranes,[14] material for gas separation applications,[15] spreadable coating materials,[16] capacitors,[17] composites[18] and nanomaterials,[19] urban mining,[20] metallurgy[21] and polymer processing.[22,23]

Received: November 30, 2013
Revised: June 30, 2014
Published: August 13, 2014

Table 1. Binary Mixtures of the $[PF_6]$-Based Compounds Studied[a]

	1					
2	$[C_3mpy]^+$	$[C_3mpyr]^+$	$[C_3mpip]^+$	$[C_{12}mim]^+$	$[N_{4444}]^+$	$[P_{4444}]^+$
$[C_3mim]^+$	√	√	√	√	√	√
$[C_3mpy]^+$		√	√			
$[C_3mpyr]^+$			√			

[a]Compounds **1** and **2** of the mixture are indentified by their cations.

Despite their broad applicability, the melting behavior of ionic mixtures is poorly known.[6] In this work, seven compounds with different cations and hexafluorophosphate ($[PF_6]^-$) as a common anion were considered for the characterization of the melting profile of nine binary mixtures of the type $[A][PF_6] + [B][PF_6]$, described in Table 1. Through the experimental measurement of the solid−liquid equilibrium (SLE) phase diagrams by optical microscopy, the main purpose of this work was to develop new ILs of the type $[A]_x[B]_{(1-x)}[PF_6]$,[3] whose melting points are lower than room temperature, using ILs/salts with high melting points.

This work is also aimed at assessing the nonideality of the liquid phase of the mixtures studied. The solid−liquid equilibrium is probably the easiest approach to assess the activity coefficients of each of the compounds in IL mixtures due to their very low volatility. For that purpose, a classical thermodynamic approach using the values of the pure compounds' melting temperatures, T_{fus} and enthalpies, $\Delta_{fus}H$ as well as their polymorphic forms' thermal transitions, T_{tr} and $\Delta_{tr}H$, determined here by differential scanning calorimetry, was used to evaluate the nonideality of the mixture liquid phase. The activity coefficients were assessed by the differences between the calculated behavior of an ideal liquid phase and the actual experimental phase behavior. This approach provides an insight on the chemical interactions in the liquid phase among the molecular structures of the compounds. The chemical structures of the studied ionic compounds as well as their abbreviations are sketched in Figure 1.

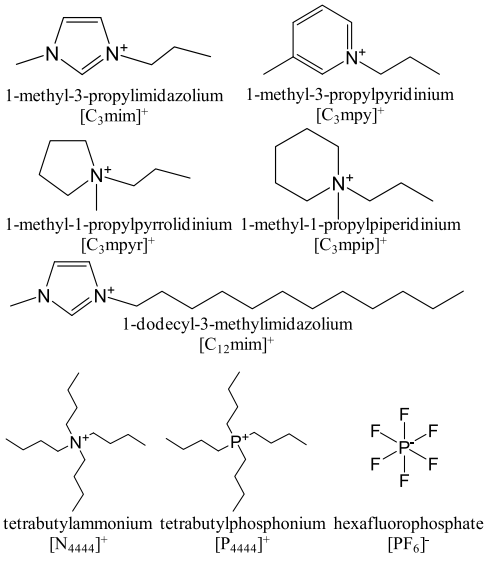

Figure 1. Chemical structures of the studied cations and the common anion $[PF_6]^-$ anion in the evaluated binary mixtures.

EXPERIMENTAL SECTION

The compounds used in this work for the preparation of the binary systems were purchased from IoLiTec (Heilbronn, Germany), except $[N_{4444}][PF_6]$ that was from Appolo Scientific (Bredbury, UK) and $[P_{4444}][PF_6]$ from Fluka (Buchs, Switzerland), with mass fraction purities higher than 99%. Pure compounds were dried under high vacuum (10^{-5} Pa) at moderate temperature (303.15 K) for at least 48 h prior to the analyses. Their water contents were verified by Karl Fisher titration (Mettler Toledo DL32), and the purity was confirmed by ^1H, ^{13}C, ^{19}F, and ^{31}P NMR spectra. All the compounds presented mass fraction purities higher than 99.5%. For the measurement of the solid−liquid phase diagrams, binary mixtures were prepared from x_1 = (0.0 to 1.0) mole fraction of compound **1**, and whose uncertainty was estimated to be $\sigma_x = 5 \times 10^{-4}$ mole fraction, by weighing 1.0000 g of the mixture in an analytical balance (Mettler Toledo, Columbus, USA) with an uncertainty of $\pm 1 \times 10^{-4}$ g. Systems were mixed by stirring, under an atmosphere of nitrogen, at 10 K above the highest melting temperature of the two compounds of the binary, until reaching the complete melting of the sample, and sequentially, cooled to atmosphere temperature. Pure compounds and their mixtures were stored under a vacuum.

Samples of the pure compounds, and some selected mixtures, were submitted to differential scanning calorimetry (DSC) using a Q200 calorimeter (TA Instruments, New Castle, USA) at ambient pressure for melting enthalpy and temperature determination. The DSC was previously calibrated with primary calibration standards, indium, naphthalene, and cyclohexane, with weight fraction purities higher than 0.99, and at a heating rate of 1 K min^{-1}. Samples of about 5 mg were tightly sealed in hermetic aluminum pans. All compounds were submitted to three repeated cycles of cooling and heating at 1 K·min^{-1} from T = 183.15 K to a temperature higher than the melting point. Thermograms of some samples, showing the three repeated cycles, are presented in Supporting Information (SI). In general, the first cycle showed slight differences regarding solid−solid transition temperatures and enthalpies due to the thermal history of the sample. A constant nitrogen flow of 50 cm^3·min^{-1} was supplied to the DSC cell in order to avoid condensation of water at the lower temperatures. The properties were measured in the last heating run, and melting temperatures were taken as the peak top values. The uncertainties of the melting temperatures and enthalpies were estimated according to the standard deviations of replicates of the pure compounds and those selected mixtures and taken as 0.50 K for melting temperatures and 0.18 kJ mol^{-1} for melting enthalpies..

The melting behavior of the pure compounds and their mixtures was studied by temperature controlled optical microscopy using a BX51 Olympus microscope (Olympus Co., Tokyo, Japan) coupled with a LTS120 temperature controller (Linkam Scientific Instruments Ltd., Tadworth, UK) ranging from 243.15 to 393.15 K with a precision of ±0.05 K. The method consisted of a heating run at 0.1 K·min^{-1} in order to reach a quasi-equilibrium state, starting by an isothermal treatment at T = 243.15 K for crystallization of the sample until reaching the complete melting. A small amount of samples, with approximately 1.0 mg, was placed in concave glass slides in order to favor the thermal transfer in the heating process by the contact of solid particles with the molten phase. The uncertainty of the melting temperatures T of the pure compounds and binary mixtures obtained by microscopy was estimated to be not higher than σ_T = 1.30 K. This value was determined according to the mean values obtained by the evaluation of at least three replicates of the pure compounds and

dx.doi.org/10.1021/cg500655s | Cryst. Growth Des. 2014, 14, 4270−4277

Table 2. Melting and Solid−Solid Transition Temperatures and Melting Enthalpies of the Studied Compounds[a]

	T_{fus}/K	$\Delta_{fus}H$/kJ·mol^{-1}	T_{tr1}/K	$\Delta_{tr1}H$/kJ·mol^{-1}	T_{tr2}/K	$\Delta_{tr2}H$/kJ·mol^{-1}
$[C_3mim][PF_6]$	311.84	14.26				
$[C_{12}mim][PF_6]$	326.31	25.88				
$[C_3mpy][PF_6]$	312.07	12.64				
$[C_3mpyr][PF_6]$	382.53	3.41	359.53	2.31	346.60	2.81
$[C_3mpip][PF_6]$	368.45	5.11	352.38	2.74	311.68	8.08
$[N_{4444}][PF_6]$	520.85	13.02	356.06	5.80	300.44	1.78
$[P_{4444}][PF_6]$	497.46	13.18	265.02	1.84		

[a]Uncertainties for melting temperatures and enthalpies are ±0.50 K and ±0.18 kJ mol^{-1}, respectively.

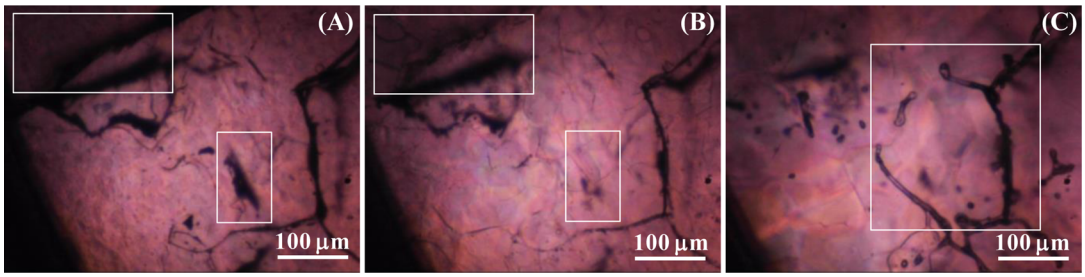

Figure 2. Micrographs of $[C_3mpyr][PF_6]$ at T = ((A) 313.15, (B) 352.65, and (C) 373.15) K. Details show changes in the surface of the crystal, during the heating of the sample.

selected binary mixtures. Moreover, melting temperatures obtained in microscopy were compared with those obtained in calorimetric measurements. The mean absolute deviations between the two techniques were always lower than the summation of the uncertainties associated with the melting temperatures obtained in microscopy and in calorimetry. Thus, the melting temperatures values for the binary mixtures obtained by the microscope could be considered as accurate.

Mixtures exhibiting solid solutions were further investigated through DSC measurements, following the same methodology described before and powder X-ray diffractometry using an Empyrean powder diffractometer (PANalytical, Almelo, Netherlands) at room temperature, with nickel filter, Cu−Kα radiation (λ = 1.54180 Å), Bragg−Brentano para-focusing optics configuration, step-scanned in 0.04° (2θ) at each 30 s. A standard reference material, lanthanum hexaboride powder was used for calibration of diffraction line positions and lines shapes determined through powder diffractometry. The pure compounds were also investigated by single crystal X-ray diffraction at 180 K with monochromated Mo−K$_\alpha$ radiation (λ = 0.71073 Å) on a Bruker SMART Apex II diffractometer (Bruker, Billerica, USA) equipped with a CCD area detector. Data reduction was carried out using a SAINT-NT software (Bruker, Billerica, USA), and multiscan absorption corrections were applied to all raw intensity data using the SADABS program (Bruker, Billerica, USA). The structures were solved by a combination of direct methods with subsequent difference Fourier syntheses and refined by full matrix least-squares on F^2 using the SHELX-97.[24] Anisotropic thermal parameters were used for all non-hydrogen atoms, while the C−H hydrogen atoms were refined with isotropic parameters equivalent to 1.2 times those of the atom to which they are bounded. Molecular diagrams were drawn with Mercury software (CCDC, Cambridge, UK) and are presented in Supporting Information (SI). The CCDC reference numbers for compounds $[C_3mim][PF_6]$, $[C_3mpy][PF_6]$, and $[C_3mpip][PF_6]$ are 972260, 972261, and 983509, respectively. These crystallographic data can be obtained free of charge from the Cambridge Crystallographic Data Centre via www.ccdc.cam.ac.uk/data_request/cif.

Modeling and Nonideality Assessment. Considering the usual thermodynamic approach to describe the phase equilibrium by means of the isofugacity criterion, the SLE modeling is well-established and has been since long used in literature for the description of phase diagrams.[25,26] Classically, the equation for the determination of the melting temperature of a binary system is built under suitable boundary conditions and taking into account general simplifications based on classical physicochemical behavior as described elsewhere[25−27] and presented as follows.

$$\ln \frac{x_i\gamma_i^L}{z_i\gamma_i^S} = \frac{\Delta_{fus}H}{R}\left(\frac{1}{T_{fus}} - \frac{1}{T}\right) + \sum_{tr=1}^{n}\left[\frac{\Delta_{tr}H}{R}\left(\frac{1}{T_{tr}} - \frac{1}{T}\right)\right] + \frac{\Delta_{fus}C_p}{R}\left(\frac{T_{fus}}{T} - \ln\frac{T_{fus}}{T} - 1\right) \quad (1)$$

where x_i and z_i are the mole fractions of the component i in the liquid and solid phases, respectively, γ_i^L and γ_i^S are the activity coefficients of the component i in the liquid and solid phases, respectively, T is the melting temperature (K) of the mixture, R is the universal gas constant (8.314 J·mol^{-1}·K^{-1}), T_{fus} and $\Delta_{fus}H$ are the melting temperature (K) and enthalpy (J·mol^{-1}) of component i, T_{tr} and $\Delta_{tr}H$ are the thermal transitions temperatures (K) and enthalpies (J·mol^{-1}) of the n solid−solid transitions (polymorphic forms) of the component i and $\Delta_{fus}C_p$ is the heat capacity (J·mol^{-1}·K^{-1}) of the component i at the melting tempearature T_{fus}. Considering the relative low difference between the melting temperatures of the pure components T_{fus} and mixtures T and also the absolute values of the $\Delta_{fus}C_p$ when compared with the $\Delta_{fus}H$ ones,[28−30] the term related to the heat capacity can be neglected as discussed elsewhere.[25,26,31] Moreover, if one considers that the system has a simple eutectic behavior in which pure compounds are immiscible in the solid phase, the term related to the nonideality of the component i in the solid phase is taken as $z_i\gamma_i^S = 1.0$. Furthermore, in the case of the liquid phase ideal behavior, the liquid phase activity coefficient is also taken as $\gamma_i^L = 1.0$. Assuming such behavior, the solid-liquid equilibrium (SLE) phase diagram can be predicted by means of only pure components properties described as follows.

$$\ln x_i^{id} = \frac{\Delta_{fus}H}{R}\left(\frac{1}{T_{fus}} - \frac{1}{T}\right) + \sum_{tr=1}^{n}\left[\frac{\Delta_{tr}H}{R}\left(\frac{1}{T_{tr}} - \frac{1}{T}\right)\right] \quad (2)$$

Otherwise, if one is interested in estimating the liquid phase's nonideality, this can be obtained from the difference between eq 1 and 2, assuming the formation of pure solid phases and negligible $\Delta_{fus}C_p$ term, as follows.

$$\ln \gamma_i = |\ln x_i^{id} - \ln x_i^{exp}| \quad (3)$$

RESULTS AND DISCUSSION

Pure Components Profiles. Table 2 presents the melting temperatures and enthalpies, as well as solid−solid transitions, of the compounds used in this work, obtained in this work or using DSC. For all the studied compounds, the melting temperatures are higher than room temperature (298.15 K) and, except for $[C_3mim][PF_6]$, $[C_{12}mim][PF_6]$, and $[C_3mpy][PF_6]$, all the remaining salts display at least one solid−solid transition. Such thermal transitions are related to polymorphism phenomena and could also be observed by microscopy as shown in Figure 2 where some micrographs taken during the heating process of $[C_3mpyr][PF_6]$ at temperatures below the first solid−solid transition (Figure 2A), after the first (Figure 2B) and second transitions (Figure 2C) are presented. Changes in the refraction properties of the material were clearly observed during the polymorphic transitions.

Suitable crystals of $[C_3mim][PF_6]$, $[C_{12}mim][PF_6]$, $[C_3mpy][PF_6]$, and $[C_3mpip][PF_6]$ were analyzed by single crystal X-ray diffraction. The final R values obtained together with pertinent crystallographic data are summarized in Supporting Information. The compounds $[C_3mpyr][PF_6]$ and $[C_{12}mim][PF_6]$ have been structurally reported elsewhere.[32,33] The asymmetric unit of $[C_3mim][PF_6]$, $[C_3mpy][PF_6]$, and $[C_{12}mim][PF_6]$ contains one PF_6 anion and one 1-methyl, 3-propylimidazolium, one 1-methyl, 3-propylpyridinium, or one 1-dodecyl, 3-methylimidazolium respectively, whereas the asymmetric unit of $[C_3mpip][PF_6]$ consists of two PF_6 anions, and two 1-methyl-1-propylpiperidinium cations and the asymmetric unit of $[C_3mpyr][PF_6]$ consist of five PF_6 anions and five 1-methyl-1-propylpyrrolidinium cations. The asymmetric units for the compounds whose crystal data were obtained in this work are represented in SI. For all compounds, the PF_6^- counterion interacts with cation through C−H···F weak hydrogen bonds with distances varying between 2.961(2) and 3.467(2) Å, which may play a role in the crystal lattice stabilization (see Figures S4−S7 in SI). The crystal packing of $[C_3mim][PF_6]$, $[C_3mpy][PF_6]$ show very well defined alternate cation anion layers interlinked by C−H···F hydrogen bonds. The crystal structure results show a probable direct correlation between the melting temperature, the presence of solid−solid transitions, and the volume of the asymmetric unit. It means that the higher the volume, the higher the melting temperature of the compounds as well as the tendency to the polymorphism, probably due to the increasing of the degrees of freedom of the structure to pack in different arrangements. Results also provide relevant information to define the solid−liquid equilibrium thermodynamic profile of the mixtures that will be discussed later.

Mixtures' SLE Experimental Behavior. The solid−liquid phase diagrams of the binary mixtures with experimental values obtained by optical microscopy are presented in Figure 3, with the exception of the $[C_3mpyr][PF_6]$ + $[C_3mpip][PF_6]$ mixture, that has a much different behavior and will be discussed later. The ideal *liquidus* line obtained using eq 2 is represented in full line, as well as the model results (dashed lines) that will be discussed below. The experimental melting temperatures of all the systems are reported in SI. The melting temperatures of the $[N_{4444}]^+$ and $[P_{4444}]^+$ based systems and their mixtures with $[C_3mim][PF_6]$ at mole fraction, x, of $[C_3mim][PF_6]$ lower than 0.7, are higher than the maximum temperature attainable with the microscope, which limits the range of mole fraction composition evaluated.

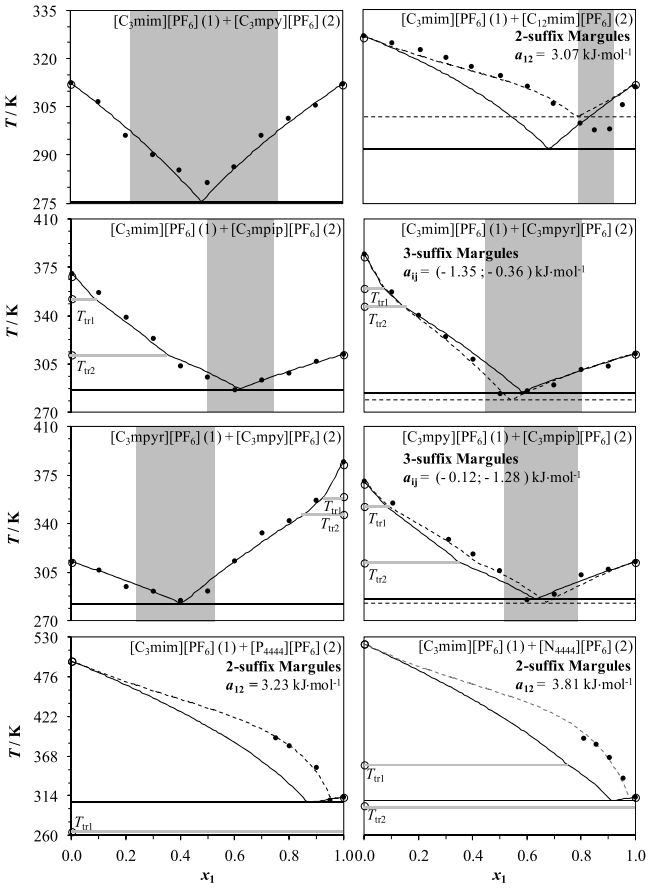

Figure 3. Solid−liquid equilibrium phase diagrams (temperature T/K versus mole fraction of the component 1, x_1) of the mixtures studied. Melting temperatures obtained by optical microscopy (●); melting and solid−solid transitions temperatures obtained by DSC (○); modeling results using eq 2 (full lines), and using eq 1 (dashed lines) but considering $x_i^S\gamma_i^S = 1.0$, neglecting the term related do $\Delta_{fus}C_p$, and using 2- or 3-suffix Margules as γ_i^L equation.[25] Gray lines represent the solid−solid transitions temperatures T_{tr1} and T_{tr2} (from Table 2). Gray regions highlight the concentration range for which the mixture is liquid at room temperature (T = 298.15 K).

All systems evaluated in Figure 3 present a eutectic-like behavior. The eutectic temperatures of the mixtures are always lower than room temperature (298.15 K), except for the tetraalkyl-based-systems. In the case of these mixtures, the eutectic concentrations, $x_{eutectic}$, are very close to the pure $[C_3mim][PF_6]$ mole fraction due to the large differences in the pure compounds' melting points. This behavior is significantly intensified by the nonideality of the system that increases the melting points of the mixtures and thwarts the possibility to obtain large melting point depressions by this approach. The greater experimental melting temperature depression obtained $T_{pure} - T_{mixture}$ = 101.50 K was observed with the $[C_3mim][PF_6]$ + $[C_3mpyr][PF_6]$ system at x_1 = 0.501 mol fraction with T = 283.15 K (see experimental SLE data in SI). The gray regions highlighted in the SLE diagrams in Figure 3 show the large concentration range in which the mixtures are in the liquid state at room temperature. Thus, considering that one of the main goals of this work was the understanding of the melting behavior of ILs' mixtures in order to decrease their melting temperature and enhance their liquid phase domain, it is possible to conclude that the decrease of the melting temperatures achieved in this work, that can be larger than 100

dx.doi.org/10.1021/cg500655s | Cryst. Growth Des. 2014, 14, 4270−4277

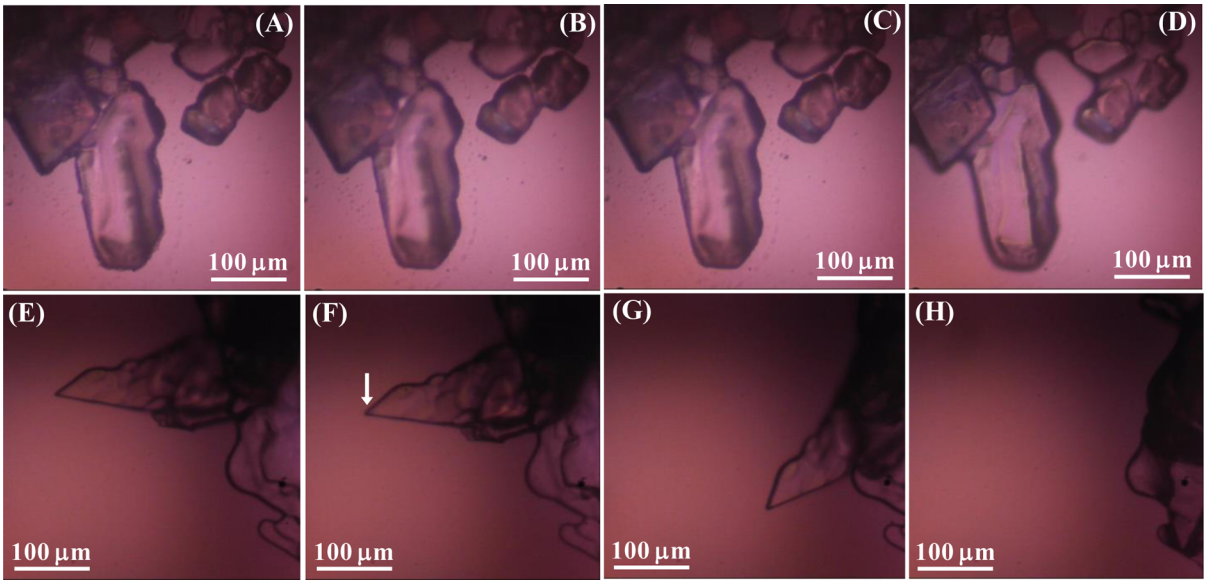

Figure 4. Micrographs of the $[C_3mim][PF_6]$ (1) + $[C_3mpy][PF_6]$ (2) system at x_1 = 0.100 mol fraction, T = ((A) 253.15, (B) 273.15, (C) 276.15, and (D) 279.15) K, and micrographs of the $[C_3mim][PF_6]$ (1) + $[C_{12}mim][PF_6]$ (2) system at x_1 = 0.104 mol fraction, T = ((E) 248.15, (F) 296.15, (G) 318.15, and (H) 323.15) K. White arrow highlight phase transition (melting) around eutectic temperature.

K by mixing mesothermal salts (ionic solids), worthily allows an extraordinary expansion of possibilities for the development of novel ILs to be used in chemical processes and product development.

Modeling the Mixtures Behavior. Considering that the systems behave as eutectic mixtures, the modeling was first attempted using eq 2, i.e., with the ideal liquid solution approach (full lines in phase diagrams of Figure 3). A modeling procedure can be useful as a tool for the prediction of the behavior of an unknown mixture. In this sense, ideal mixtures are quite relevant in the practical context because the knowledge of pure compounds properties, i.e., their melting temperature and enthalpy, as well as polymorphism/solid−solid transitions parameters are enough for a complete description of their SLE. In fact, without the need for adjustment of γ_i equations, the modeling becomes completely predictive. Works in the open literature have been showing this pattern that, from the excess properties point of view, IL mixtures behave approximately as ideal mixtures.[3,6,34−38] Since the mixtures present a eutectic behavior the solid-phase in the biphasic (solid + liquid) region is composed by pure component 2 at the left-hand side of the phase diagram and pure component 1 above the eutectic composition. This assumption is confirmed by optical micrographs presented in Figure 4. It presents the some pictures taken during the heating of mixtures of $[C_3mim][PF_6]$ + $[C_3mpy][PF_6]$ at x_1 = 0.100 and $[C_3mim][PF_6]$ + $[C_{12}mim][PF_6]$ at x_1 = 0.104. They show that, except for the $[C_3mpyr][PF_6]$ + $[C_3mpip][PF_6]$ mixture, the beginning of the melting and so the biphasic domain could be clearly identified, during the heating of the sample, at around $T \cong T_{\text{eutectic}}$ (Figure 4C) with the appearance of a liquid phase, and displacement of the crystals. This profile is observed in both regions close to the pure components ($x_1 \rightarrow 0$) and throughout the concentration range.

Moreover, a judicious evaluation of the melting parameters of the pure ILs is crucial for the accuracy of the modeling procedure. As mentioned before, except for $[C_3mim][PF_6]$ and $[C_3mpy][PF_6]$, the other compounds studied here present at least one endothermic transition before the melting temperature which is related to changes in conformational structure, i.e., polymorphic structures. This phenomenon is well-known in the ILs literature.[33,39] From the thermodynamic modeling point of view, in some cases, polymorphism is irrelevant because temperatures or enthalpies are too low to be considered, or the transition is close enough to the melting temperature to be embodied or considered as part of the melting processes. However, in this work, the magnitude of the enthalpy of the polymorphic forms' transitions is highly significant when compared to the melting enthalpy and, in a similar way, temperatures cannot be undervalued. For instance, if polymorphism is not taken into account in the ideal assumption modeling, i.e., the variables in eq 2 related to the solid−solid transitions T_{tr} and $\Delta_{tr}H$ are set to zero, the relative deviations from experimental data could increase up to 9.30% (in the $[C_3mim][PF_6]$ + $[N_{4444}][PF_6]$ system) and the *liquidus* line would suffer a significant positive deviation. Consequently, the melting temperature decrease becomes overestimated with lower eutectic temperature values. The $[C_3mim][PF_6]$ + $[C_3mpip][PF_6]$ mixture's phase diagram presented in SI exemplifies the phenomena.

In summary, qualitatively, the results here reported suggest that for mixtures of ILs with a common anion, the use of eq 2 as a predictive tool, aiming for the design of new ILs from ionic solids, is a reasonable first approach with a maximum deviation in the predicted melting temperatures lower than 9.0% for the tetraalkyl-based mixtures, and lower than 3.70% for the remaining mixtures, while deviations are below 1.9% considering the prediction of the eutectic temperature for the $[C_3mim][PF_6]$ + $[C_{12}mim][PF_6]$ asymmetric system.

Assessment on the Nonideality of the Mixtures. Notwithstanding the satisfactory predictive ability of the ideal approach in the description of the solid−liquid equilibrium behavior of most mixtures studied, only three of them can strictly be considered as ideal mixtures: $[C_3mim][PF_6]$ + $[C_3mpy][PF_6]$, $[C_3mim][PF_6]$ + $[C_3mpip][PF_6]$, and $[C_3mpyr][PF_6]$ + $[C_3mpy][PF_6]$. For the other systems, positive or negative deviations from ideal behavior were observed in which $\gamma_i^L \neq 1.0$. This can be easily checked by

dx.doi.org/10.1021/cg500655s | *Cryst. Growth Des.* 2014, 14, 4270−4277

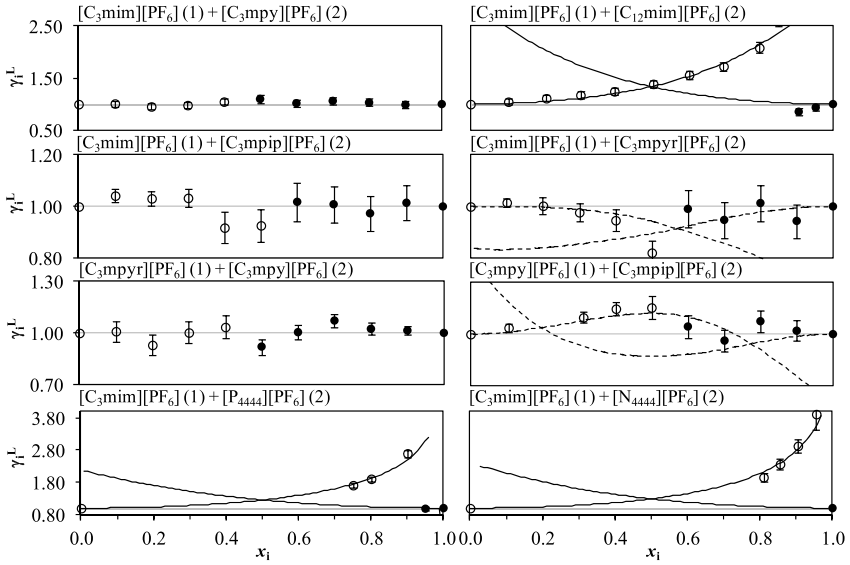

Figure 5. Liquid phase's activity coefficients of the component 1 (●) and 2 (○) calculated by eq 3 and using γ_i^L equations: 2-suffix-Margules (full lines) and 3-suffix-Margules (dashed lines). Error bars were calculated by error propagation at the 0.95 confidence level.

comparison of the experimental data and the ideal *liquidus* lines (full line) depicted in Figure 3. However, in order to evaluate the magnitude of ideality/nonideality profile of these systems, the values of γ_i^L were then calculated by eq 3 and are depicted in Figure 5.

Assuming the uncertainty of γ_i^L at the 0.95 confidence level, calculated from the experimental standard deviation on the melting properties (T_{fus}, T_{tr}, $\Delta_{tr}H$, and $\Delta_{tr}H$ in Table 2) and mole fraction x_i, the ideal profile can be, in fact, assumed for the three aforementioned systems. A different behavior is however observed for the remaining systems. For the mixture composed of $[C_3mim][PF_6]$ + $[C_3mpyr][PF_6]$, the liquid phase of both compounds presents slight negative deviations of up to 0.85. For the $[C_3mpy][PF_6]$ + $[C_3mpip][PF_6]$ system, a positive deviation is observed for the $[C_3mpip][PF_6]$, while $[C_3mpy][PF_6]$ behaves as in an ideal mixture. In any of these cases, with exception of narrow concentration regions around the eutectic point, the systems can be considered ideal within the combined uncertainty of the experimental data and the simplifying assumptions considering the heat capacities. In fact, the molecular structures of $[C_3mim][PF_6]$, $[C_3mpy][PF_6]$, $[C_3mpyr][PF_6]$, and $[C_3mpip][PF_6]$ (Figure 1) are very similar, taking into account the size of ring, differing by one carbon atom, unsaturation, and position of the radical. Moreover, crystallographic data (Supporting Information) show that all of them present monoclinic unit cells, and the same space group, with the exception of $[C_3mpyr][PF_6]$. These structural similarities support the ideal or almost ideal thermodynamic behavior of the aforementioned binaries in the liquid phase.

The three other systems present a markedly nonideal behavior. In the $[C_3mim][PF_6]$ + $[C_{12}mim][PF_6]$ system, in the narrow concentration range available $[C_3mim][PF_6]$ seems to present a negative deviation, unlike the marked positive deviation of $[C_{12}mim][PF_6]$'s liquid phase with activity coefficients of up to 2.72. This is quite interesting as the entropic contributions arising from the size differences between the two compounds would grant negative deviations to ideality, but the nanostructure of the $[C_{12}mim][PF_6]$, with completely interdigitated molecular packing (see the crystal unit cell structures of pure $[C_{12}mim][PF_6]$ in SI), as also observed elsewhere,[32,40,41] changes the expectable behavior of this system with the introduction of a second compound contributing to the disruption of that nanostructure and inducing a strong nonideality. Similarly, in the case of $[N_{4444}][PF_6]$ and $[P_{4444}][PF_6]$ with $[C_3mim][PF_6]$ mixtures, the tetraalkyl-based ILs also present marked positive deviations, but since eutectic points are very close to pure $[C_3mim][PF_6]$, the equilibrium region related to this compound is too small to allow the identification of any significant deviation from ideal behavior. In this example, the differences in the dominant interactions between the aliphatic tetraalkyl cations and the aromatic imidazolium cations can explain their system nonideality. By using the 2- or 3-suffix Margules equation for the calculation of the γ_i^L the phase behavior could be well-described in all nonideal cases (see model results in dashed lines in Figure 3) except for the $[C_3mim][PF_6]$ + $[C_{12}mim][PF_6]$ system. In this case, the high deviations do not allow a good description of the eutectic point. In fact, the values of the γ_i^L calculated by eq 3 and presented in Figure 5 show that this is the most nonideal system followed by the tetraalkyl-based mixtures.

Curious Case of the $[C_3mpyr][PF_6]$ + $[C_3mpip][PF_6]$ Alloy. The system composed of $[C_3mpyr][PF_6]$ + $[C_3mpip][PF_6]$ and for which the respective phase diagram is presented in Figure 6 displays a unique behavior, with a very unusual noneutectic profile that was additionally evaluated by DSC and powder X-ray diffractometry of the solid phase. The thermograms and diffractograms are reported in SI. The DSC melting temperature profile is in close agreement with that measured by optical microscopy. Simple eutectic mixtures present two endothermic transitions during the melting process, one related to the eutectic reaction and the other related to the melting.[42−45] However, the thermograms of this system present a single endothermic transition, which suggests the presence of a continuous solid solution and formation of an alloy. Solid solutions are a state where the two compounds crystallize on a single crystal lattice, and the solid phase can be considered as a monophasic system. The formation of a monophasic alloy was confirmed by powder X-ray analysis (SI). In the case of immiscibility, mixtures should present diffraction peaks at the

dx.doi.org/10.1021/cg500655s | Cryst. Growth Des. 2014, 14, 4270−4277

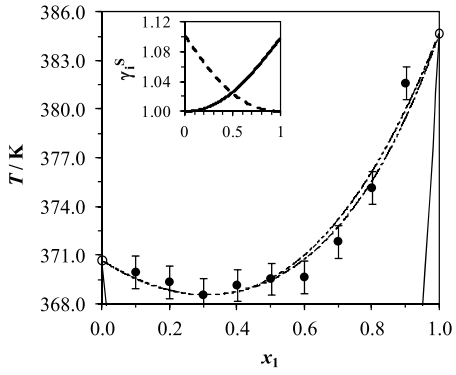

Figure 6. Solid–liquid equilibrium phase diagram of the [C_3mpyr][PF_6] (1) + [C_3mpip][PF_6] (2) mixture with experimental data obtained by optical microscopy (●) or by DSC (○). Model results considering $\gamma_i^L = 1.0$ and $x_i^S\gamma_i^S = 1.0$ (dashed lines), and considering $\gamma_i^L = 1.0$ and $\gamma_i^S \neq 1.0$ using 2-suffix-Margules equation (solid lines) with binary interaction parameter a_{ij} = 0.30 kJ·mol^{-1}. In detail, γ_i^S of component 1 (dashed line) and component 2 (solid line). Error bars with the uncertainty for T, σ_T = 1.30 K.

same scattering angles of the two pure compounds. Still, the diffractograms show that the mixtures' patterns changed quickly from those of pure [C_3mpip][PF_6] (2) to those of pure [C_3mpyr][PF_6] (1) at x_1 = 0.05, remaining at this value during the entire concentration range. The SLE phase diagram can thus be described as a continuous solid solution in the entire concentration range where the [C_3mpip][PF_6] is incorporated as a guest on the [C_3mpyr][PF_6] crystalline lattice. This is probably due to the similarities in the crystallographic structure of the two pure compounds.[46−48] In fact, an assessment on single crystal X-ray data (SI) of pure [C_3mpyr][PF_6] and [C_3mpip][PF_6] shows that both ILs have a very similar monoclinic unit cell regarding the crystallographic axes angles. Moreover, the crystal packing of [C_3mpyr][PF_6] presents 36 formular units per unit cell, whereas [C_3mpip][PF_6] presents only 8. This means that, comprising very different crystal volumes, the crystalline structure of [C_3mpyr][PF_6] can probably act as a host-structure to accommodate the crystal structure of [C_3mpip][PF_6] leading to the formation of the alloy.

The SLE modeling of a system with solid phase nonideality and miscibility requires that $z_i\,\gamma_i^S \neq 1.0$. In this case, given the similarity of the two compounds and the results obtained above, for the modeling of the phase diagram it was assumed that the nonideality of this mixture is only due to the solid phase, and the 2-suffix-Margules equation was used for the description of the activity coefficient of the solid phase γ_i^S. Figure 6 presents the phase diagram of such system comprising both *liquidus* and *solidus* lines. This γ_i model was chosen because even with just one single adjustable parameter a_{ij} the description of the experimental data is as accurate as obtained for the other systems. The calculated phase diagram shows a homogeneous azeotrope-type shape with a minimum point close to x_1 = 0.340 [C_3mpyr][PF_6] mole fraction and a narrow biphasic region, i.e., $x_i \cong z_i$. This profile is in agreement with a positive deviation from ideality[49] (see inset in Figure 4).

CONCLUSIONS

The results reported in this work show that it is possible to prepare IL mixtures, with melting temperatures lower than room temperature based on mesotherm salts and thus allowing the design of new ILs. The behavior of most of the binary mixtures can be closely predicted by assuming an ideal liquid phase behavior through the correct values of the pure compounds melting properties and other solid–solid transitions. While most of the systems studied present ideal behavior, or close to ideal liquid phases, it is shown that large differences in the alkyl chain length or in the cation nature may induce important liquid phase nonideality.

The system [C_3mpyr][PF_6] + [C_3mpip][PF_6] presents a curious behavior displaying the formation of a continuous solid solution that is a quite rare phenomenon among organic compounds. To the best of our knowledge, this is one of the few IL alloys ever reported and the first detailed crystallographic characterization of such an alloy. The overall physicochemical/melting profiles described here that further investigations on solid–liquid equilibrium of ILs and mesotherm salts are important as they can be an important tool to assess the nonideality of the liquid phase of these mixtures, allowing researchers to probe the nature of the molecular interactions. They disclose, moreover, an important approach to the design of IL mixtures based on compounds of high melting points that may enlarge the range of available ILs.

ASSOCIATED CONTENT

Supporting Information

Tables with crystal data and selected refinement details for the compounds [C_3mim][PF_6], [C_{12}mim][PF_6], [C_3mpy][PF_6], [C_3mpy][PF_6], and [C_3mpip][PF_6], experimental solid–liquid equilibrium data, DSC thermograms and powder X-ray diffractograms of the [C_3mpyr][PF_6] + [C_3mpip][PF_6] mixture, solid–liquid equilibrium phase diagram for the [C_3mim][PF_6] + [C_3mpip][PF_6] system with and without polymorphic transitions, crystalline structures of [C_3mim][PF_6], [C_{12}mim][PF_6], [C_3mpy][PF_6], and [C_3mpyr][PF_6] and their crystallographic files (CIF), and DSC thermograms for pure compounds. This material is available free of charge via the Internet at http://pubs.acs.org.

AUTHOR INFORMATION

Corresponding Author

*Fax: + 351 234 370 084; Tel: + 351 234 401 507; E-mail: jcoutinho@ua.pt.

Notes

The authors declare no competing financial interest.

ACKNOWLEDGMENTS

The authors are grateful to the national funding agencies FAPESP (2012/05027-1, 2008/56258-8), CNPq (483340/2012-0, 140718/2010-9, 406856/2013-3), and CAPES (BEX-13716/12-3) from Brazil and FCT (Projects Pest-C/CTM/LA0011/2013, Pest-OE/EQB/LA0004/2011 and contracts under Investigator FCT program (JMSSE and MGF)) from Portugal for the financial support.

REFERENCES

(1) Brennecke, J. F.; Maginn, E. J. *AIChE J.* **2001**, *47*, 2384−2389.
(2) Wilkes, J. S. *Green Chem.* **2002**, *4*, 73−80.
(3) Niedermeyer, H.; Hallett, J. P.; Villar-Garcia, I. J.; Hunt, P. A.; Welton, T. *Chem. Soc. Rev.* **2012**, *41*, 7780−7802.
(4) Zhang, Y.; Maginn, E. J. *J. Chem. Theory Comput.* **2013**, *9*, 1592−1599.

(5) Reichert, W. M.; Holbrey, J. D.; Swatloski, R. P.; Gutowski, K. E.; Visser, A. E.; Nieuwenhuyzen, M.; Seddon, K. R.; Rogers, R. D. *Cryst. Growth Des.* **2007**, *7*, 1106−1114.
(6) Lopes, J. N. C.; Cordeiro, T. C.; Esperanca, J.; Guedes, H. J. R.; Huq, S.; Rebelo, L. P. N.; Seddon, K. R. *J. Phys. Chem. B* **2005**, *109*, 3519−3525.
(7) Baltazar, Q. Q.; Leininger, S. K.; Anderson, J. L. *J. Chromatogr. A* **2008**, *1182*, 119−127.
(8) Wang, H.; Gurau, G.; Rogers, R. D. *Chem. Soc. Rev.* **2012**, *41*, 1519−1537.
(9) Freire, M. G.; Teles, A. R. R.; Ferreira, R. A. S.; Carlos, L. D.; Lopes-da-Silva, J. A.; Coutinho, J. A. P. *Green Chem.* **2011**, *13*, 3173−3180.
(10) Long, J.; Guo, B.; Li, X.; Jiang, Y.; Wang, F.; Tsang, S. C.; Wang, L.; Yu, K. M. K. *Green Chem.* **2011**, *13*, 2334−2338.
(11) Gorlov, M.; Kloo, L. *Dalton T.* **2008**, 2655−2666.
(12) Lane, G. H.; Bayley, P. M.; Clare, B. R.; Best, A. S.; MacFarlane, D. R.; Forsyth, M.; Hollenkamp, A. F. *J. Phys. Chem. C* **2010**, *114*, 21775−21785.
(13) Raade, J. W.; Padowitz, D. *J. Sol. Energy Eng.* **2011**, 133.
(14) Lin, B.; Dong, H.; Li, Y.; Si, Z.; Gu, F.; Yan, F. *Chem. Mater.* **2013**, *25*, 1858−1867.
(15) Voss, B. A.; Bara, J. E.; Gin, D. L.; Noble, R. D. *Chem. Mater.* **2009**, *21*, 3027−3029.
(16) Voss, B. A.; Noble, R. D.; Gin, D. L. *Chem. Mater.* **2012**, *24*, 1174−1180.
(17) Lewandowski, A.; Galiński, M. *J. Phys. Chem. Solids* **2004**, *65*, 281−286.
(18) Snedden, P.; Cooper, A. I.; Scott, K.; Winterton, N. *Macromolecules* **2003**, *36*, 4549−4556.
(19) Tunckol, M.; Durand, J.; Serp, P. *Carbon* **2012**, *50*, 4303−4334.
(20) Kondo, H.; Matsumiya, M.; Tsunashima, K.; Kodama, S. *Electrochim. Acta* **2012**, *66*, 313−319.
(21) Wellens, S.; Goovaerts, R.; Möller, C.; Luyten, J.; Thijs, B.; Binnemans, K. *Green Chem.* **2013**, *15*, 3160−3164.
(22) Soll, S.; Zhao, Q.; Weber, J.; Yuan, J. *Chem. Mater.* **2013**, *25*, 3003−3010.
(23) Yuan, J.; Giordano, C.; Antonietti, M. *Chem. Mater.* **2010**, *22*, 5003−5012.
(24) Sheldrick, G. *Acta Crystallogr. A* **2008**, *64*, 112−122.
(25) Reid, R. C.; Prausnitz, J. M.; Pouling, B. E. *The Properties of Gases and Liquids*; McGraw-Hill: New York, 1987.
(26) Gmehling, J.; Kolbe, B.; Kleiber, M.; Rarey, J. *Chemical Thermodynamics for Process Simulation*; Wiley-VHC: Weinheim, 2012.
(27) Prausnitz, J. M.; Lichtenthaler, R. N.; Azevedo, E. G. *Molecular Thermodynamics of Fluid-Phase Equilibria*; Prentice-Hall: NJ, 1986.
(28) Gardas, R. L.; Coutinho, J. A. P. *Ind. Eng. Chem. Res.* **2008**, *47*, 5751−5757.
(29) Diedrichs, A.; Gmehling, J. *Fluid Phase Equilib.* **2006**, *244*, 68−77.
(30) Paulechka, Y. U. *J. Phys. Chem. Ref. Data* **2010**, *39*, 033108−23.
(31) Coutinho, J. A. P.; Andersen, S. I.; Stenby, E. H. *Fluid Phase Equilib.* **1995**, *103*, 23−39.
(32) Gordon, C. M.; Holbrey, J. D.; Kennedy, A. R.; Seddon, K. R. *J. Mater. Chem.* **1998**, *8*, 2627−2636.
(33) Golding, J.; Hamid, N.; MacFarlane, D. R.; Forsyth, M.; Forsyth, C.; Collins, C.; Huang, J. *Chem. Mater.* **2001**, *13*, 558−564.
(34) D'Anna, F.; Marullo, S.; Vitale, P.; Noto, R. *ChemPhysChem* **2012**, *13*, 1877−1884.
(35) Stoppa, A.; Buchner, R.; Hefter, G. *J. Mol. Liq.* **2010**, *153*, 46−51.
(36) Shimizu, K.; Tariq, M.; Rebelo, L. P. N.; Canongia Lopes, J. N. *J. Mol. Liq.* **2010**, *153*, 52−56.
(37) Aparicio, S.; Atilhan, M. *J. Phys. Chem. B* **2012**, *116*, 2526−2537.
(38) Navia, P.; Troncoso, J.; Romani, L. *J. Chem. Eng. Data* **2007**, *52*, 1369−1374.
(39) MacFarlane, D. R.; Meakin, P.; Sun, J.; Amini, N.; Forsyth, M. *J. Phys. Chem. B* **1999**, *103*, 4164−4170.
(40) Canongia Lopes, J. N. A.; Pádua, A. A. H. *J. Phys. Chem. B* **2006**, *110*, 3330−3335.
(41) Russina, O.; Triolo, A. *Faraday Discuss.* **2012**, *154*, 97−109.
(42) Costa, M. C.; Rolemberg, M. P.; Boros, L. A. D.; Krähenbühl, M. A.; de Oliveira, M. G.; Meirelles, A. J. A. *J. Chem. Eng. Data* **2007**, *52*, 30−36.
(43) Maximo, G. J.; Costa, M. C.; Meirelles, A. J. A. *Braz. J. Chem. Eng.* **2013**, *30*, 33−43.
(44) Annat, G.; Forsyth, M.; MacFarlane, D. R. *J. Phys. Chem. B* **2012**, *116*, 8251−8258.
(45) Sun, J.; Forsyth, M.; MacFarlane, D. R. *J. Phys. Chem. B* **1998**, *102*, 8858−8864.
(46) Stott, P. W.; Williams, A. C.; Barry, B. W. *J. Controlled Release* **1998**, *50*, 297−308.
(47) Leuner, C.; Dressman, J. *Eur. J. Pharm. Biopharm.* **2000**, *50*, 47−60.
(48) Chiou, W. L.; Riegelma, S. *J. Pharm. Sci.* **1971**, *60*, 1281−1302.
(49) Ricci, J. E. *The Phase Rule and Heterogeneous Equilibrium*; Dover Publications: New York, 1966.